

## OPEN ACCESS

# Multi-frequency Operation of a MEMS Vibration Energy Harvester by Accessing Five Orders of Parametric Resonance

To cite this article: Y Jia *et al* 2013 *J. Phys.: Conf. Ser.* **476** 012126

View the [article online](#) for updates and enhancements.

## Related content

- [Parametric resonance for vibration energy harvesting with design techniques to passively reduce the initiation threshold amplitude](#)  
Yu Jia, Jize Yan, Kenichi Soga *et al.*
- [Parametrically excited MEMS vibration energy harvesters with design approaches to overcome the initiation threshold amplitude](#)  
Yu Jia, Jize Yan, Kenichi Soga *et al.*
- [Modelling of a bridge-shaped nonlinear piezoelectric energy harvester](#)  
G Gafforelli, R Xu, A Corigliano *et al.*

## Recent citations

- [A Numerical Feasibility Study of Kinetic Energy Harvesting from Lower Limb Prosthetics](#)  
Yu Jia *et al*
- [Real world assessment of an auto-parametric electromagnetic vibration energy harvester](#)  
Yu Jia *et al*
- [Development of MEMS Multi-Mode Electrostatic Energy Harvester Based on the SOI Process](#)  
Bongwon Jeong *et al*



**IOP | ebooks™**

Bringing you innovative digital publishing with leading voices to create your essential collection of books in STEM research.

Start exploring the collection - download the first chapter of every title for free.

# Multi-frequency Operation of a MEMS Vibration Energy Harvester by Accessing Five Orders of Parametric Resonance

Y Jia, J Yan, K Soga and A A Seshia

Department of Engineering, University of Cambridge, Cambridge CB2 1PZ, UK

E-mail: yj252@cam.ac.uk

**Abstract.** The mechanical amplification effect of parametric resonance has the potential to outperform direct resonance by over an order of magnitude in terms of power output. However, the excitation must first overcome the damping-dependent initiation threshold amplitude prior to accessing this more profitable region. In addition to activating the principal (1st order) parametric resonance at twice the natural frequency  $\omega_0$ , higher orders of parametric resonance may be accessed when the excitation frequency is in the vicinity of  $2\omega_0/n$  for integer  $n$ . Together with the passive design approaches previously developed to reduce the initiation threshold to access the principal parametric resonance, vacuum packaging ( $< 10$  torr) is employed to further reduce the threshold and unveil the higher orders. A vacuum packaged MEMS electrostatic harvester ( $0.278 \text{ mm}^3$ ) exhibited 4 and 5 parametric resonance peaks at room pressure and vacuum respectively when scanned up to  $10 \text{ g}$ . At  $5.1 \text{ ms}^{-2}$ , a peak power output of  $20.8 \text{ nW}$  and  $166 \text{ nW}$  is recorded for direct and principal parametric resonance respectively at atmospheric pressure; while a peak power output of  $60.9 \text{ nW}$  and  $324 \text{ nW}$  is observed for the respective resonant peaks in vacuum. Additionally, unlike direct resonance, the operational frequency bandwidth of parametric resonance broadens with lower damping.

## 1. Introduction

In addition to the conventional use of direct resonance for resonant-based vibration energy harvesting, parametric resonance has been previously demonstrated as a potential superior resonant mechanism in terms of peak power attainable at certain conditions [1]. Instead of yielding a forced response, parametric resonant build-up arises from a periodic modulation in one of the system parameters. The principal (1st order) parametric resonance can be activated around twice the natural frequency. Moreover, the same system is theoretically predicted to possess several higher orders of parametric resonance at  $2\omega_0/n$ , where  $\omega_0$  is the natural frequency and  $n$  is a positive integer representing the order number of parametric resonance. The unveiling of these higher orders introduces additional operational frequency bands across the power spectrum. However, the onset of the higher parametric orders is less trivial due the rapid narrowing of the instability regions [2] as can be seen from the Strutt diagram of the damped Mathieu equation (Equation 1) shown in Figure 1.

$$\ddot{x} + c\dot{x} + (\delta + 2\varepsilon \cos(2t))x = 0 \quad (1)$$

where  $x$  is displacement,  $c$  is damping,  $\delta$  is squared of natural frequency,  $\varepsilon$  is excitation amplitude,  $t$  is time while assuming unit mass. The shaded unstable areas in the Strutt diagram represent the parametric regimes. Upon activation, the oscillatory amplitude growth is not bounded by linear damping and only saturates due to nonlinearities at high amplitudes.



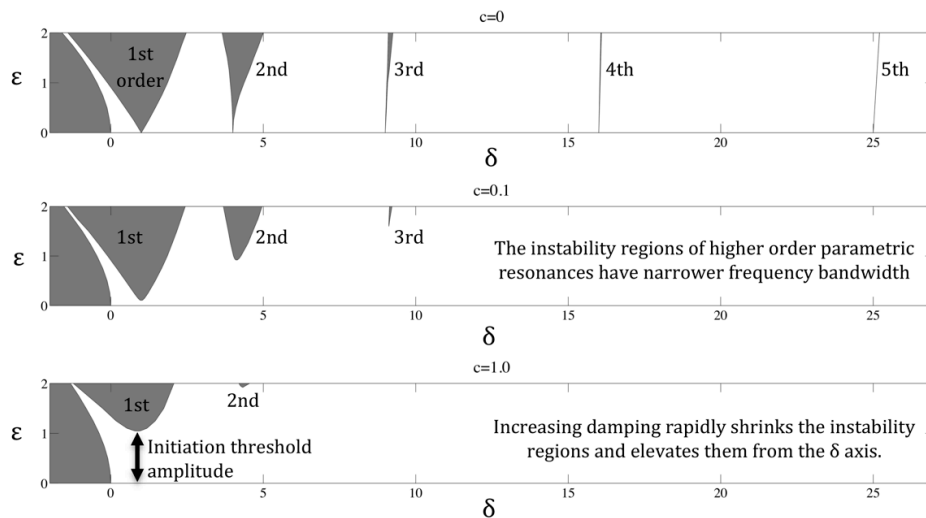


**Figure 1.**  $\delta$ - $\epsilon$  plane stability chart for the Mathieu equation (Strutt diagram) showing up to 5 orders. Shaded instability areas represent achievement of parametric resonance.

The system response for all orders of parametric resonance is always near the natural frequency despite the distinct respective excitation frequencies. However, the accessibility of the higher orders is increasingly difficult with higher damping as a result of both the rise of the damping-dependent initiation threshold amplitude that the excitation must minimally attain and the ever-narrowing frequency bandwidth. Therefore, the higher order instability regions rapidly shy away from the base axis with increasing damping as seen in figure 1. Damping due to air drag, which typically dominates the damping in MEMS devices at atmospheric pressure, is directly related to the cross-sectional area of the shuttle and the body-shape-dependent drag coefficient. Air drag for comb finger structures is relatively smaller than that for gap-closing plate configurations and the relative accessibility of higher order instability regions in MEMS parametric resonators has been previously demonstrated [3].

**2. Apparatus**

The electrostatic harvester employed for this investigation can be seen in figures 2 and 3. The shuttle consists of a cantilever beam with an array of capacitive comb fingers running off its sides. The supposedly anchored end of the cantilever is coupled to the centre of an orthogonal clamped-clamped beam, which acts as the initial spring for the amplification of the base excitation that is fed into the parametric resonator (the cantilever). This threshold-aid design has been previously shown to decrease the initiation threshold of an otherwise sole cantilever structure by over an order of magnitude [1].

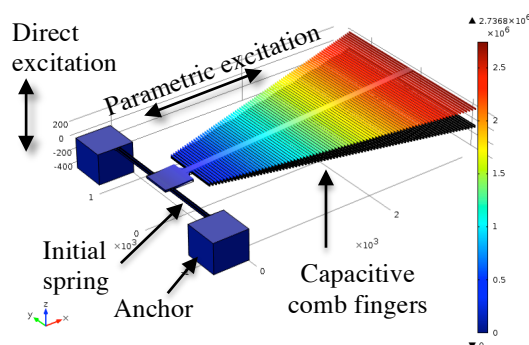


**Figure 2.** Harvester design with initial spring to reduce initiation threshold.

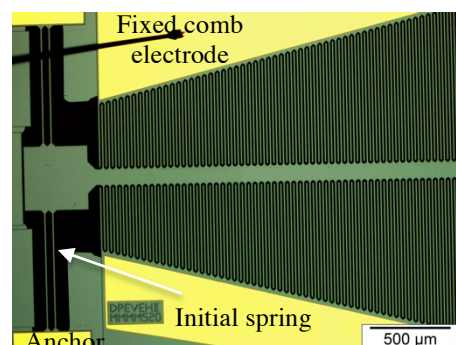


**Figure 3.** Optical micrograph of the MEMS harvester prototype.

The active device, with 0.278 mm<sup>3</sup> device and anchor volume, 25 μm thick device silicon, is driven on a mechanical shaker with the free end of the resonator positioned upright to help overcome the non-zero initial displacement criterion for activating parametric resonance from an orthogonal excitation. An acceleration scan of up to 10 g was carried out for the predicated frequency vicinities of the fundamental mode of direct resonance as well as the various orders of parametric resonance.

In addition to operation in atmospheric pressure conditions, the device was also vacuum packaged (pressure < 10 torr) with an in-house procedure to reduce damping as shown in figure 4. The vacuum pressure is a conservative estimate extrapolated from the quality factor of a MEMS double-ended tuning fork located on the same chip. Figure 5 shows the laser vibrometer scan of the direct resonant response of the device around the natural frequency (COMSOL<sup>®</sup> eigenfrequency simulated to be ~303.9 Hz). The out-of-plane direct resonant peak showed an increase in quality factor from ~1.5 in room pressure to ~9 with the decreased damping inside the vacuum seal.

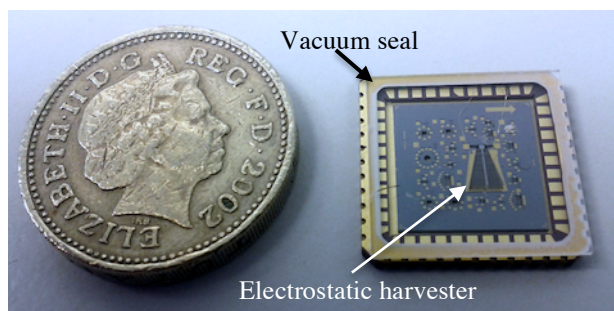


**Figure 4.** Vacuum packaged device.

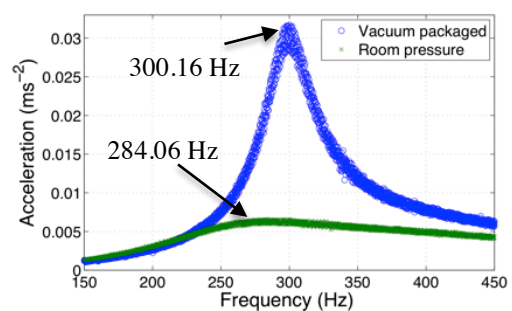


**Figure 5.** Vibrometer scan ~  $f_n$ .

### 3. Result

#### 3.1. Initiation threshold amplitude

The initiation threshold for various resonant peaks and their power response per excitation acceleration is given by table 1 and figure 6. At room pressure, the first four orders of parametric resonance onset at 1.57 ms<sup>-2</sup>, 2.45 ms<sup>-2</sup>, 3.24 ms<sup>-2</sup> and 4.22 ms<sup>-2</sup> respectively; while in vacuum, five orders of parametric resonance were uncovered at noticeably lower initiation thresholds of 0.98 ms<sup>-2</sup>, 1.64 ms<sup>-2</sup>, 2.62 ms<sup>-2</sup>, 3.92 ms<sup>-2</sup> and 13.73 ms<sup>-2</sup> respectively. No other higher order resonant peaks were recorded up to 10 g of acceleration. Upon activating a parametric resonant regime, the power output rapidly outraces the direct resonant response with increasing excitation.

Table 1. Peak power output, half power bandwidth (HPB) and initiation threshold amplitude (ITA) of the fundamental direct mode and first 5 parametric orders of the prototype in room and vacuum pressure conditions; ‘n/r’ denotes not recorded and ‘n/a’ denotes not applicable.

Resonant peaks	Room pressure			Vacuum packaged		
	Driven at 5.1 ms <sup>-2</sup>			Driven at 5.1 ms <sup>-2</sup>		
	Power (nW)	HPB (Hz)	ITA (ms <sup>-2</sup> )	Power (nW)	HPB (Hz)	ITA (ms <sup>-2</sup> )
1st mode	20.8	40	n/a	60.9	11	n/a
1st order	166	80	1.57	324	160	0.98
2nd order	105	21	2.45	259	35	1.64
3rd order	67	7	3.24	175	9.8	2.62
4th order	22	2.7	4.22	84	3.5	3.92
5th order	n/r	n/r	n/r	0	0	13.73

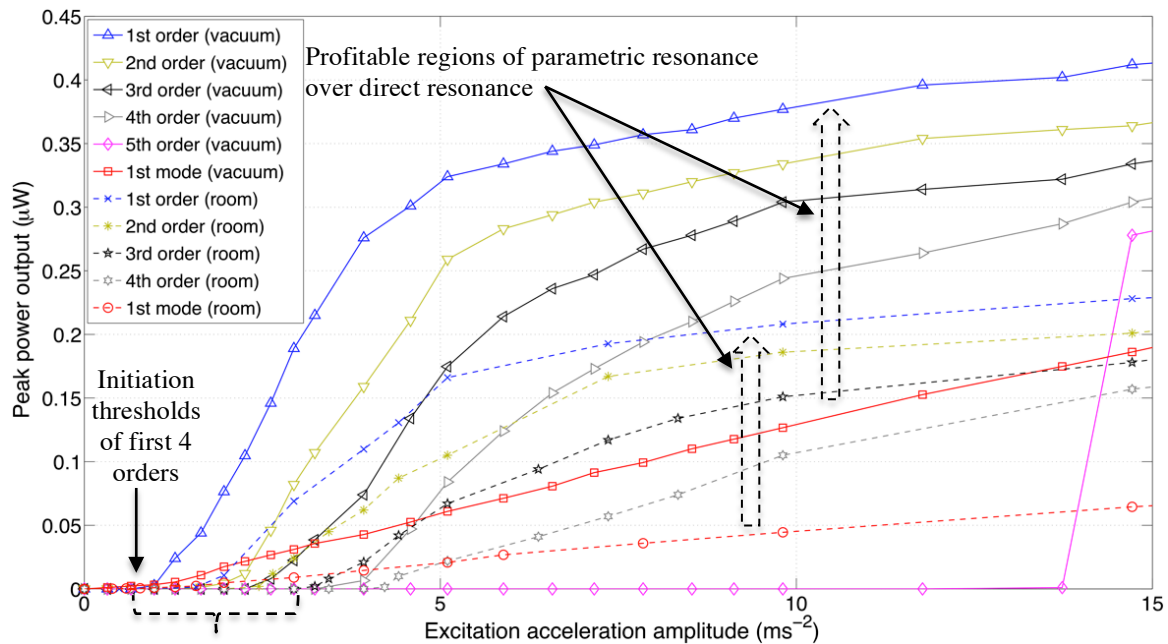


**Figure 6.** Experimental power response versus excitation acceleration. The initiation thresholds of parametric resonance decrease with lower damping in vacuum.

Although supplementary operational frequency regions from the higher orders were observed, only the principal order parametric resonance was relatively easy to access along with the direct resonant response. The second order overlaps with the fundamental mode and a timed modulation between the linear harmonic and parametric motion takes place, which usually returns to the direct resonant regime. The third and higher orders have significantly narrower frequency bandwidth and longer transient build-up time ( $> 1$  minute). Therefore, the higher orders are only practical for very specific and non-time variant excitation frequencies.

The onset of the additional fifth parametric order for the vacuum packaged device was at significantly higher amplitude than that of the first four orders and the power response rapidly attained a high level upon accessing the parametric regime. This implies a lower true initiation threshold exists for the fifth order and the potential presence of further higher orders for both atmospheric pressure operation and vacuum packaged devices within the scanned acceleration range; however, these additional instability regions have been experimentally elusive due to the impractically narrow operational frequency bandwidth for the frequency sweeps to reveal. To accommodate the prolonged transient build-up time of the parametric regimes, manual frequency sweeps with frequency holds for each individual frequency point were carried out. Therefore, the tedious experimental procedure could have missed these narrow peaks, if they existed.

### 3.2. Power and frequency

Table 1 and figure 7 present the power peaks and frequency bandwidth for an input acceleration level of  $5.1 \text{ ms}^{-2}$ . The power peaks and half power bands at atmospheric pressure for direct resonance and principal parametric resonance were  $20.8 \text{ nW}$  and  $40 \text{ Hz}$ , and  $166 \text{ nW}$  and  $80 \text{ Hz}$  respectively; while that for vacuum were  $60.9 \text{ nW}$  and  $11 \text{ Hz}$  and  $324 \text{ nW}$  and  $160 \text{ Hz}$  respectively. The higher parametric orders exhibited rapidly-narrowing bandwidth as can be seen from the logarithmic frequency scale of figure 1. The lower attainable peaks for the higher orders are a result of the system operating at relatively less dominant parts of the instability regions for the given boundary conditions.

For direct resonance, despite the increase of power output in vacuum from the lower damping, the frequency bandwidth is sacrificed as expected. This narrowing in operational frequency with increasing sensitivity has become synonymous with higher quality factor (ratio of energy stored and

energy dissipated). In the case of parametric resonance however, as damping decreases, the frequency bandwidth broadens along with the increase in power peak and quality factor. This is a result of the unstable tongues (Figure 1) approaching the horizontal base axis and the system moving deeper into the dominant parts of the instability region.

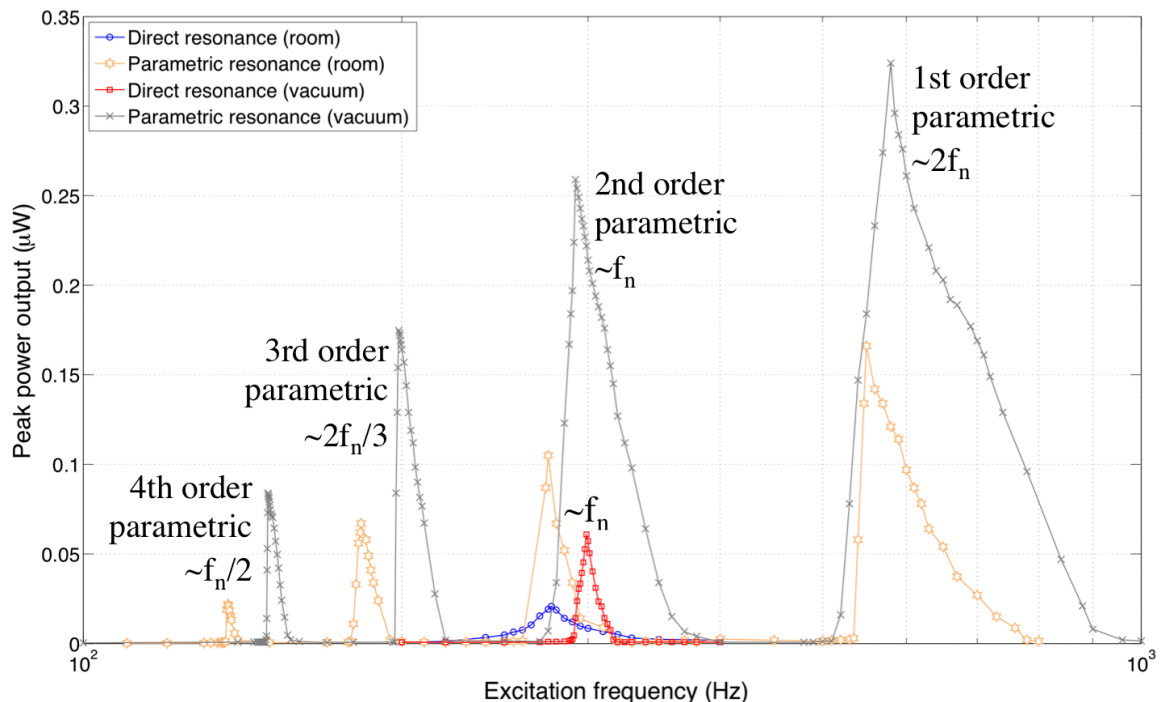


**Figure 7.** Power spectrum for acceleration of  $5.1 \text{ ms}^{-2}$ . Note the logarithmic scale for frequency.

This also implies lower initiation threshold and onset of the profitable regions at lower excitation levels as shown in figure 6. Lower initiation threshold also yields easier accessibility for the higher orders of parametric resonance. Nonetheless, the fast narrowing of the frequency bands at higher orders still provides an experimental and practical challenge for accessibility despite their theoretical presence. The drift of the resonant frequency with time further adds to the difficulty of rediscovering these hard to locate frequency bands with their strict combination of boundary conditions.

## Conclusion

A MEMS electrostatic harvester was driven into direct resonance and various orders of parametric resonance. The device in room pressure experimentally revealed 4 orders of parametric resonance while the vacuum packaged scenario uncovered the 5th order as well. With lower damping in vacuum, the parametric peaks experienced both power increase and frequency broadening. Coupled with the initial spring structure previously investigated, the vacuum packaged parametrically excited harvester demonstrated the onset of the profitable regions over direct resonance for an input acceleration of  $1 \text{ ms}^{-2}$ . Future work involves design of structures with minimal air drag and higher quality vacuum packaging to further improve the accessibility of the various orders of parametric resonance.

## References

- [1] Jia Y, Yan J, Soga K and Seshia A A 2012 *Proc. PowerMEMS 2012* (Atlanta) pp. 215-218
- [2] Levy D M and Keller J B 1963 *Commun. Pure Appl. Math.* **16** pp. 469-476
- [3] Turner K L, Miller S A, Hartwell P G, MacDonald N C, Strogatz S H and Adams S G 1998 *Lett. Nature* **396** pp. 149-152